

Communication: Vibrational and vibronic coherences in the two dimensional spectroscopy of coupled electron-nuclear motion

Cite as: J. Chem. Phys. **143**, 041102 (2015); <https://doi.org/10.1063/1.4927396>

Submitted: 28 May 2015 . Accepted: 14 July 2015 . Published Online: 24 July 2015

Julian Albert , Mirjam Falge, Sandra Gomez, Ignacio R. Sola, Heiko Hildenbrand, and Volker Engel



View Online



Export Citation



CrossMark

ARTICLES YOU MAY BE INTERESTED IN

[Electron-nuclear wave-packet dynamics through a conical intersection](#)

The Journal of Chemical Physics **146**, 074304 (2017); <https://doi.org/10.1063/1.4975811>

[Communication: Adiabatic and non-adiabatic electron-nuclear motion: Quantum and classical dynamics](#)

The Journal of Chemical Physics **144**, 171103 (2016); <https://doi.org/10.1063/1.4948777>

[Two-dimensional Fourier transform electronic spectroscopy at a conical intersection](#)

The Journal of Chemical Physics **140**, 124312 (2014); <https://doi.org/10.1063/1.4867996>

Lock-in Amplifiers

... and more, from DC to 600 MHz



Watch



Communication: Vibrational and vibronic coherences in the two dimensional spectroscopy of coupled electron-nuclear motion

Julian Albert,¹ Mirjam Falge,¹ Sandra Gomez,² Ignacio R. Sola,² Heiko Hildenbrand,¹ and Volker Engel¹

¹Universität Würzburg, Institut für Physikalische und Theoretische Chemie, Emil-Fischer-Str. 42, Campus Nord, Am Hubland, 97074 Würzburg, Germany

²Departamento de Química Física, Universidad Complutense, 28040 Madrid, Spain

(Received 28 May 2015; accepted 14 July 2015; published online 24 July 2015)

We theoretically investigate the photon-echo spectroscopy of coupled electron-nuclear quantum dynamics. Two situations are treated. In the first case, the Born-Oppenheimer (adiabatic) approximation holds. It is then possible to interpret the two-dimensional (2D) spectra in terms of vibrational motion taking place in different electronic states. In particular, pure vibrational coherences which are related to oscillations in the time-dependent third-order polarization can be identified. This concept fails in the second case, where strong non-adiabatic coupling leads to the breakdown of the Born-Oppenheimer-approximation. Then, the 2D-spectra reveal a complicated vibronic structure and vibrational coherences cannot be disentangled from the electronic motion. © 2015 AIP Publishing LLC. [<http://dx.doi.org/10.1063/1.4927396>]

Two-dimensional (2D) optical spectroscopy^{1–5} is, by now, an established technique of molecular spectroscopy.^{6–14} Regarding, for example, coupled chromophores as purely electronic systems, 2D-spectra exhibit cross-peaks and thus reveal properties of excited state electronic coupling. The issue becomes much more complicated if vibrations are included in the considerations. It was shown theoretically that already for a model of two displaced harmonic oscillators, cross peaks appear so that their pure existence is no unique sign of electronic coupling.¹⁵ Several experiments have addressed the role of vibrational motion.^{16–21} In this context the question of vibrational versus electronic coherences and their signatures in 2D-spectra was discussed also from a theoretical point of view.^{22,23} It is the aim of the present work to perform a theoretical test study to shed some light on such concepts. In order to do so, it is necessary to treat the coupled electron-nuclear motion, preferentially by solving the time-dependent Schrödinger equation for the entire system under consideration. This, however, is out of range for molecules. It is therefore useful to introduce models which, on one hand, fully account for electron-nuclei coupling and, on the other, are simple enough to be treated numerically exact. Such a model was proposed by Shin and Metiu,²⁴ and it has served to illustrate fundamental properties of electron-nuclear dynamics in the past.^{25–27}

The Shin-Metiu model describes the one-dimensional motion of an electron (coordinate x) and a proton (coordinate R). Additionally, there are two protons fixed at distances ± 5 Å from the origin of the coordinate system. The geometry of the ion chain is sketched in the upper panel of Fig. 1. The electron and the nuclei interact through screened Coulomb potentials (screening parameter R_c), whereas the bare Coulomb potential is kept for the nuclear interactions.²⁴ The eigenenergies of the model Hamiltonian $H_0(x, R)$ are denoted as E_α . Potential energy curves $V_n(R)$ in different electronic states $|n\rangle$ with electronic wave functions $\varphi_n(x, R)$ are obtained

from the electronic Schrödinger equation for fixed R . Within the Born-Oppenheimer (BO) approximation,²⁸ the nuclear motion in a fixed electronic state $|n\rangle$ is determined by the nuclear Hamiltonian $H^n(R)$ containing the potential $V_n(R)$ and having energies $E_{n,v}$.

The potentials for electronic quantum numbers $n = 1–4$ are shown in Fig. 1. The functions in the lower panel of the figure are obtained for a screening parameter of $R_c = 1.5$ Å. It is seen that the electronic ground state $|1\rangle$ is energetically well separated from the first excited state. The first two excited states $|2\rangle$ and $|3\rangle$ are closer in energy but still are separated by a gap of about 0.5 eV at $R = 0$, whereas the curve of state $|4\rangle$ is much higher in energy. The energy separation of the various curves suggests that the BO-approximation is valid, and wave-packet calculations show that this indeed is the case.^{25,26} The situation changes if we set $R_c = 2.5$ Å (middle panel of Fig. 1). Then, the potentials of the ground and first excited states approach each other very closely at the symmetric configuration $R = 0$. This leads to a complete break down of the BO-approximation.^{25,26}

We numerically integrate the time-dependent Schrödinger equation for the coupled motion including the electric dipole interaction $(-\mu(x, R)E(t))$, with $\mu(x, R) = -x + R$ and the electric field $E(t)$. For comparison, we treat the nuclear motion within the BO-approximation, where the nuclear dynamics in two electronic states is only coupled by the field interaction $(-\mu_{nm}(R)E(t))$, with the transition dipole moments $\mu_{nm}(R) = \langle \varphi_n(x, R) | \mu(x, R) | \varphi_m(x, R) \rangle_x$. The electric field interacting with the system consists of three time-delayed and time-ordered Gaussian pulses (\vec{k}_n) with equal frequency which are centered at times T_n . This allows to define the coherence time $\tau = T_2 - T_1$ and the population time $T = T_3 - T_2$. Taking the phase-matching condition $\vec{k}_s = -\vec{k}_1 + \vec{k}_2 + \vec{k}_3$ (where \vec{k}_s denotes the wave vector of the signal field) into account, the third-order time-dependent polarization has two contributions

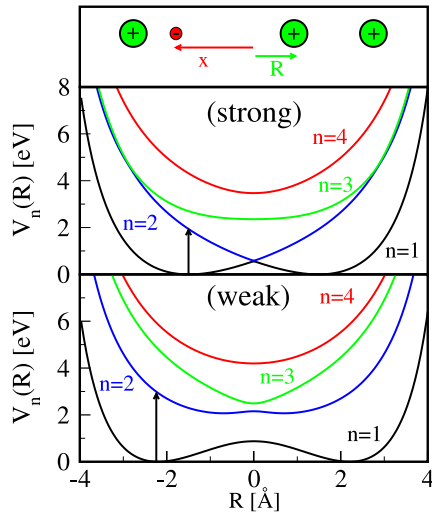


FIG. 1. Upper panel: Geometry of the model system. Potential energy curves $V_n(R)$ for different electronic states $|n\rangle$ and the strong and weak coupling cases are also shown. The arrows indicate the photon energies used in the respective numerical calculations.

and can be written as

$$P^{(c)}(t', \tau, T) = \langle \psi^{(2)}(k_2, k_1) | \mu | \psi^{(1)}(k_3) \rangle_{x,R} + \langle \psi^{(2)}(k_3, k_1) | \mu | \psi^{(1)}(k_2) \rangle_{x,R}, \quad (1)$$

where the detection-time t' is measured with respect to the time T_3 . Here, we neglect contributions involving excited state absorption because we want to compare two-state Born-Oppenheimer results with those obtained within the numerically exact calculation. Also, the complex conjugate of the two terms are omitted because they are not calculated explicitly. The wave-functions $\psi^{(2)}(k_l, k_1)$ and $\psi^{(1)}(k_l)$ are obtained within second- and first-order time-dependent perturbation theory, where the first one results from the combined interaction with the pulses (k_l, k_1) and the second from the absorption process triggered by pulse (k_l) . These functions are calculated iteratively²⁹ for a set of sampling times t'_j and τ_j . We use $N_{t'} = N_\tau = 7000$ points taken from the intervals $[10, 345]$ fs for τ and $[0, 335]$ fs for t' .

In the calculations involving the adiabatic approximation, the fields couple the electronic states $|1\rangle$ and $|2\rangle$, and the polarization reads

$$P^{(BO)}(t', \tau, T) = \langle \psi_1^{(2)}(k_2, k_1) | \mu_{12} | \psi_2^{(1)}(k_3) \rangle + \langle \psi_1^{(2)}(k_3, k_1) | \mu_{12} | \psi_2^{(1)}(k_2) \rangle, \quad (2)$$

where $\psi_1^{(2)}(k_l, k_1)$ are ground-state and $\psi_2^{(1)}(k_l)$ excited state vibrational wave packets, respectively.

The 2D-spectrum ($s = c, BO$) is calculated as³⁰

$$S^s(E_{t'}, E_\tau, T) = i \int d\tau \int dt' e^{i(E_{t'}t' - E_\tau\tau)} P^{(s)}(t', \tau, T). \quad (3)$$

For interpretation, the polarizations can be written in terms of the system eigenstates.^{31–33} The resulting expression for $P^{(c)}$ contains sums over the quantum numbers $(\alpha, \alpha', \alpha'')$ where terms with different time-dependent phase factors appear which

read

$$e^{i(E_{\alpha'} - E_\alpha)t'} e^{i(E_{\alpha''} - E_0)\tau} e^{i(E_{\alpha'} - E_0)T}, \quad (4)$$

$$e^{i(E_{\alpha'} - E_\alpha)t'} e^{i(E_{\alpha''} - E_0)\tau} e^{i(E_{\alpha''} - E_\alpha)T}.$$

In the BO-approximation, one finds (summation over (v, v', v''))

$$e^{i(E_{1,v} - E_{2,v'})t'} e^{i(E_{2,v''} - E_{1,0})\tau} e^{i(E_{1,v} - E_{1,0})T}, \quad (5)$$

$$e^{i(E_{1,v} - E_{2,v'})t'} e^{i(E_{2,v''} - E_{1,0})\tau} e^{i(E_{2,v''} - E_{2,v'})T}.$$

In both cases, oscillations are found where the periods are determined by differences between eigenenergies. At this point, it is important to emphasize that a single quantum number characterizes the coupled system so that the appearing energies are not associated with vibrational levels in electronic states. On the other hand, in the BO-case, energy differences between vibrational eigenenergies in the excited and ground electronic states (in phases containing t', τ) and differences of vibrational energies in a single electronic state (in phases containing T) enter. For long enough sampling times, the 2D-spectra will exhibit peaks at positions $(E_{t'} = E_{\alpha'} - E_\alpha, E_\tau = E_{\alpha''} - E_0)$ and $(E_{t'} = E_{1,v} - E_{2,v'}, E_\tau = E_{2,v''} - E_{1,0})$.

In what follows, we compare 2D-spectra calculated exactly, that is, solving numerically the Schrödinger equation without any approximation which decouples electronic and nuclear motion, with those evolving from a Born-Oppenheimer treatment where the vibrational motion in two electronic states is only coupled by the laser fields. Figure 2 shows the spectra for the weak coupling. To arrive at a broad spectrum, we employ ultrashort pulses of 2.8 fs full width at half-maximum and a photon energy of 2.9 eV. The population time T is set to zero. A comparison of the spectra shows that they are almost identical which confirms that here the BO-treatment is valid. We may then use Eq. (5) and associate the peak positions with energy differences between the vibrational levels in the excited and ground electronic states. The wave packets which enter into the third-order polarization perform a ground-state ($\psi_1^{(2)}$) and an excited state ($\psi_2^{(1)}$) vibrational motion. In the ground state, three pairs of nearly degenerate gerade and ungerade levels are excited. The wave packet moves, for short times, with a vibrational period of about 58 fs. In the excited state, 20 vibrational states are present in the wave packet and the period is ≈ 50 fs. Because all energy differences between the various levels appear in the time-dependent polarization, the 2D-spectrum exhibits the rich peak structure.

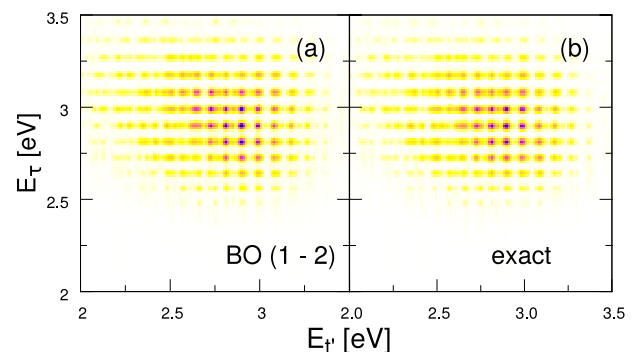


FIG. 2. Modulus of the Born-Oppenheimer and exact 2D-spectrum (normalized) for weak coupling ($R_c = 1.5$ Å).

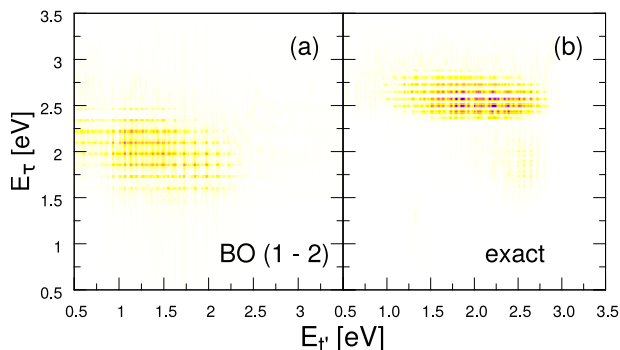


FIG. 3. Modulus of the Born-Oppenheimer and exact 2D-spectrum (normalized) for the strong coupling case ($R_c = 2.5 \text{ \AA}$).

Next, we turn to the strong coupling case. Here, we use a photon energy of 1.9 eV for all pulses. The exact spectrum (panel (b) of Figure 3) exhibits an intense band around $E_T = 2.6 \text{ eV}$. Regarding the potential energy curves in Fig. 1, it can be assumed that this band involves transitions to the electronic state $|3\rangle$. This is confirmed in calculating the respective BO-spectrum (not shown) which very much resembles the exact spectrum at energies above $E_T' = 2 \text{ eV}$. Transitions between vibrational states in $|1\rangle$ and $|2\rangle$ are also present in the exact spectrum but the peaks are of comparably small intensity. This can already be seen in the linear absorption spectrum³⁴ (not shown) and correlates with the magnitude of the transition dipole moment. The BO-spectrum (panel (a)) shows no resemblance with the exact one which is a manifestation of the breakdown of the adiabatic approximation.

The polarizations show oscillations as a function of the population time T (Eqs. (4) and (5)). To illustrate this point, we regard the functions $P^{(s)}(t_f', \tau = 0, T)$ which are cuts through the polarizations obtained for zero coherence time and a fixed value of $t' = t_f' = 10 \text{ fs}$. Taking the Fourier-transform with respect to T yields the spectra $S^s(E_T)$ shown in Fig. 4. As found for the 2D-spectra, the BO and exact curves are very similar in the weak coupling case (left panels). Regarding the analytical expressions, Eqs. (4) and (5), we can clearly identify the spectral lines as being of purely vibrational character, i.e., they are caused by coherences which belong to the vibrational motion in the excited and also the ground electronic state. The right hand panels of Fig. 4 illustrate the strong coupling situation and it is seen that the spectra do not match each other. This means that here the coherences obtained as a function of the population time can no longer be associated with the vibrational dynamics in fixed electronic states. Rather, they are characterized by energy differences $(E_{\alpha'} - E_0), (E_{\alpha'} - E_{\alpha})$ which are of a strongly mixed vibrational/electronic character.

Let us add some more words on the distinction between electronic and vibrational coherences. Molecular photoexcitation with ultrashort pulses leads, in general, to vibronic wave packets. There might be the case that such an interaction results in no vibrational excitation. Then, one could argue that the field-coupled states and the associated coherences are of purely electronic character. The Franck-Condon principle demands that ground and excited state potential surfaces have to be very similar in order that no vibrations are excited in a spectro-

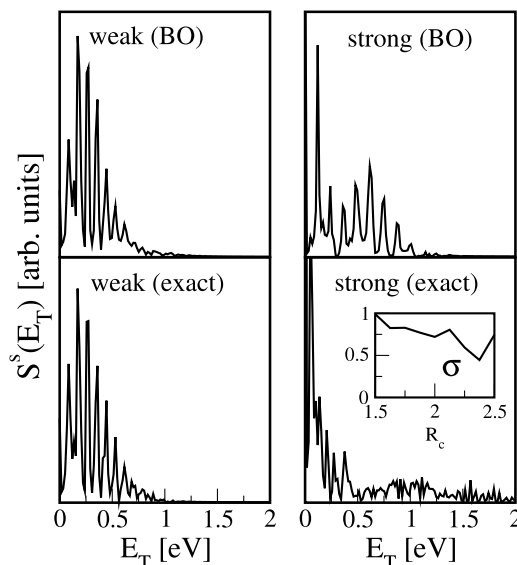


FIG. 4. Spectra calculated from the third-order polarization determined as a function of the population time T and for fixed coherence- and detection time. Curves are shown for the cases of strong ($R_c = 2.5 \text{ \AA}$) and weak ($R_c = 1.5 \text{ \AA}$) couplings. The inset in the lower right panel shows the spectral overlap between the BO- and exact spectra as a function of the screening parameter R_c .

scopic transition. This is, however, very unlikely for larger molecules or molecular aggregates. As discussed above, it is possible to characterize vibrational coherences within a fixed electronic state if the BO-approximation holds. It would then be desirable to find a measure for the characterization—at least theoretically. Therefore, we regard the spectral overlap $\sigma = N \int dE_T S^{BO}(E_T) S^c(E_T)$, where the normalization constant N is chosen such that, if the spectra are identical, i.e., the BO-approximation is valid, σ assumes the value of one. The larger the deviation between the spectra, the smaller the spectral overlap so that σ gives an overall measure of the quality of the adiabatic approximation. The inset in Fig. 4 (lower right panel) shows σ as a function of the screening parameter R_c . As expected, for $R_c = 1.5 \text{ \AA}$, we obtain a value of one. Increasing this critical parameter yields to a decrease of the overlap function and a minimum is reached for a value of $R_c = 2.375 \text{ \AA}$.

To conclude, we regard the 2D-spectroscopy of a model consisting of an electron and a nucleus which move in a single dimension. By adjusting the screening of the particle interaction, a situation with weak and strong non-adiabatic couplings can be constructed. In the first case, the Born-Oppenheimer approximation is valid. This allows to identify coherences appearing in the third-order time-dependent polarization as a function of the population time T as being of purely vibrational character. The break-down of the adiabatic approximation, however, forbids such an assignment because electronic and nuclear dynamics are strongly mixed. This means that the coherences are associated with energies which are of vibronic character and thus cannot be assigned to particular electronic states. In this sense, purely electronic coherences are unlikely to be excited. It is just that either the separation of electronic and nuclear motion can be performed and one is able to assign certain oscillations to vibrations in particular electronic states

or, for stronger coupling, one just has to give up the ambition to find a meaningful disentanglement. We here study a simple model of coupled electronic-nuclear motion which nevertheless has all the ingredients to demonstrate the influence of non-adiabatic coupling on 2D-spectra. Regarding the spectroscopy of molecular aggregates like self-aggregating dyes in solution or photosynthetic systems, the breakdown of the BO-approximation is more the rule than the exception. This can already be taken from an analysis of the topology of the potential surfaces for a dimer aggregate including vibrations.³⁵ There, if the electronic couplings are in the order of the vibrational spacings, no separation into electronic or vibrational coherences is possible.

The financial support by the DFG (Grant No. FOR 1809) and the COST-action (Grant No. CM1204, XLIC) is gratefully acknowledged.

- ¹J. D. Hybl, A. W. Albrecht, S. M. G. Faeder, and D. M. Jonas, *Chem. Phys. Lett.* **297**, 307 (1998).
- ²P. Tian, D. Keusters, Y. Suzuki, and W. S. Warren, *Science* **300**, 1553 (2003).
- ³M. L. Cowan, J. P. Ogilvie, and R. J. D. Miller, *Chem. Phys. Lett.* **386**, 184 (2004).
- ⁴T. Brixner, T. Mančal, I. Stiopkin, and G. R. Fleming, *J. Chem. Phys.* **121**, 4221 (2004).
- ⁵T. Brixner, J. Stenger, H. M. Vaswani, M. Cho, R. E. Blankenship, and G. R. Fleming, *Nature* **434**, 625 (2005).
- ⁶G. S. Engel, T. R. Calhoun, E. L. Read, T.-K. Ahn, T. Mančal, Y.-C. Cheng, R. E. Blankenship, and G. R. Fleming, *Nature* **446**, 782 (2007).
- ⁷A. Nemeth, F. Milota, T. Mančal, V. Lukes, H. F. Kauffmann, and J. Sperling, *Chem. Phys. Lett.* **459**, 94 (2008).
- ⁸E. L. Read, G. S. Schlau-Cohen, G. S. Engel, J. Wen, R. E. Blankenship, and G. R. Fleming, *Biophys. J.* **95**, 847 (2008).
- ⁹J. A. Myers, K. L. M. Lewis, F. D. Fuller, P. F. Tekavec, C. F. Yocum, and J. P. Ogilvie, *J. Phys. Chem. Lett.* **1**, 2774 (2010).
- ¹⁰M. Kullmann, S. Ruetzel, J. Buback, P. Nuernberger, and T. Brixner, *J. Am. Chem. Soc.* **133**, 13074 (2011).
- ¹¹O. Bixner, V. Lukes, T. Mančal, J. Hauer, F. Milota, M. Fischer, I. Pugliesi, M. Bradler, W. Schmid, E. Riedle *et al.*, *J. Chem. Phys.* **136**, 204503 (2012).
- ¹²D. Hayes, G. B. Griffin, and G. S. Engel, *Science* **340**, 1431 (2013).
- ¹³S. Ruetzel, M. Diekmann, P. Nuernberger, C. Walter, B. Engels, and T. Brixner, *Proc. Natl. Acad. Sci. U. S. A.* **111**, 4764 (2014).
- ¹⁴S. Mukamel and H. J. Bakker, "Preface: Special topic on multidimensional spectroscopy," *J. Chem. Phys.* **142**, 212101 (2015).
- ¹⁵D. Egorova, M. F. Gelin, and W. Domcke, *J. Chem. Phys.* **126**, 074314 (2007).
- ¹⁶A. Nemeth, F. Milota, T. Mančal, V. Lukeš, J. Hauer, H. F. Kauffmann, and J. Sperling, *J. Chem. Phys.* **132**, 184514 (2010).
- ¹⁷T. Mančal, A. Nemeth, F. Milota, V. Lukeš, H. F. Kauffmann, and J. Sperling, *J. Chem. Phys.* **132**, 184514 (2010).
- ¹⁸D. B. Turner, K. E. Wilk, P. M. G. Curmi, and G. D. Scholes, *J. Phys. Chem. Lett.* **2**, 1904 (2011).
- ¹⁹K. Franstedt and G. S. Engel, *Chem. Phys.* **403**, 59 (2012).
- ²⁰V. Tiwari, W. K. Peters, and D. M. Jonas, *PNAS* **110**, 1203 (2013).
- ²¹A. Halpin, P. J. M. Johnson, R. Tempelaar, R. S. Murphy, J. Knoester, T. Jansen, and R. J. D. Miller, *Nat. Chem.* **6**, 196 (2014).
- ²²J. Yuen-Zhou, J. J. Kirch, and A. Aspuru-Guzik, *J. Chem. Phys.* **136**, 234501 (2012).
- ²³M. B. Plenio, J. Almeida, and S. F. Huelga, *J. Chem. Phys.* **139**, 235102 (2013).
- ²⁴S. Shin and H. Metiu, *J. Chem. Phys.* **102**, 9285 (1995).
- ²⁵M. Erdmann, P. Marquetand, and V. Engel, *J. Chem. Phys.* **119**, 672 (2003).
- ²⁶M. Falge, V. Engel, and S. Gräfe, *J. Phys. Chem. Lett.* **3**, 2617 (2012).
- ²⁷F. Agostini, A. Abedi, Y. Suzuki, S. K. Min, N. T. Maitra, and E. K. U. Gross, *J. Chem. Phys.* **142**, 084303 (2015).
- ²⁸M. Born and K. Huang, *Theory of Crystal Lattices* (Oxford University Press, London, 1954).
- ²⁹V. Engel, *Comput. Phys. Commun.* **63**, 228 (1991).
- ³⁰P. Kjellberg, B. Brüggemann, and T. Pullerits, *Phys. Rev. B* **74**, 024303 (2006).
- ³¹D. M. Jonas, *Annu. Rev. Phys. Chem.* **54**, 425 (2003).
- ³²A. Schubert and V. Engel, *J. Chem. Phys.* **134**, 104304 (2011).
- ³³D. Egorova, *J. Chem. Phys.* **140**, 034314 (2014).
- ³⁴M. Erdmann and V. Engel, *J. Chem. Phys.* **120**, 158 (2004).
- ³⁵W. J. D. Beenken, M. Dahlbom, P. Kjellberg, and T. Pullerits, *J. Chem. Phys.* **117**, 5810 (2002).